

## CdO Nanoparticles: Facile Synthesis and Influence of Particle Size on Photocatalytic Degradation of Methylene Blue

\*D.J. Jeejamol<sup>1</sup>, A. Moses Ezhil Raj<sup>1</sup>, K. Jayakumari<sup>2</sup>, C. Ravidhas<sup>3</sup>

<sup>1</sup>(Department of Physics & Research Centre, Scott Christian College (Autonomous),  
Nagercoil – 629 003, India)

<sup>2</sup>(Department of Physics, Sree Ayyappa College for Women, Chunkankadai – 629 807, India)

<sup>3</sup>(PG & Research Department of Physics, Bishop Heber College (Autonomous), Tiruchirappalli – 620 017,  
India)

Corresponding Author: D.J. Jeejamol

---

**Abstract:** Present work attempts to share the properties of the semiconducting cadmium oxide nanoparticles synthesized by the co-precipitation method, so as to cope with waste water treatment through photocatalysis. As-prepared Cd(OH)<sub>2</sub> sample was calcined and the temperatures were prefixed based on the results of thermogravimetry (TG) and differential thermal analysis (DTA). The crystal structure and the crystallite size were estimated from the X-ray diffraction patterns and were confirmed through transmission electron microscope. The hexagonal and spherical morphology, whose sizes in the range 22 to 72 nm exhibited the presence of more active sites suitable for the photocatalytic process. The optical band gaps calculated in the range 2.2 to 2.5 eV informed the viability of the materials to initiate photocatalytic reaction in the visible light region. Particle size dependent photocatalytic activities were assessed by studying the photo degradation of methylene blue dye. The percentage of color abatement in the aqueous solution for 5 hours was good for the sample calcined at 400 °C (71%). The degradation rate of methylene blue followed the pseudo-first order kinetics and the rate constant obtained was in the range 0.2975 to 0.3474 hr<sup>-1</sup>.

**Keywords:** co-precipitation, semiconducting oxide, photocatalytic, transmission electron microscope

---

Date of Submission: 03-08-2017

Date of acceptance: 13-09-2017

---

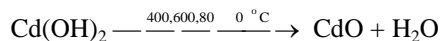
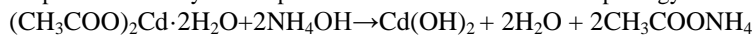
### I. Introduction

Discharging toxic contaminants from industries such as textiles, food, paper, cosmetics and so on into the environment requires refining and therefore various techniques such as coagulation, flocculation, membrane filtration, photocatalytic degradation etc. have been used to eliminate coloured contaminants. Discharged waste water from textile industry is contaminated mainly with dyes that consume oxygen and thus affect the aquatic life [1]. Methylene blue (MB) is one such cationic dye, extensively used for dyeing cloth would cause severe carcinogenic and mutagenic effects to human beings and wildlife. Therefore, the removal of MB is essentially a challenging task to protect the environment. One of the most effective and applicable methods for the elimination of environmental pollutants is the photocatalytic degradation process in which nanoparticles has been used in view of solar energy utilization that results two different electron transfer quenching path-ways, i.e. reductive or oxidative quenching [2].

Thanks to the growth of nanoscience and nanotechnology for providing ample techniques for the production of nanoparticles. Scientists have investigated many semiconductors that consume visible light to degrade a large number of recalcitrant materials in aqueous system and as a matter of fact nano-sized metal oxide semiconductor materials gained a wide-reaching recognition as the preferable compounds for purification of water [3]. Different type of metal oxide semiconductors such as, ZnO [4], SnO<sub>2</sub> [5], TiO<sub>2</sub> [6], few metal particles Ag [7], Au [8], Pd [9], Pt [10] and few doped metal oxides [11] have been used widely to degrade organic pollutants. Studies have been already initiated to degrade methylene blue using palladium and gold dendrimer [12], La doped ZnO nanoflowers [13], ZnO/Ag/CdO nanocomposite [14] and polyaniline/CdO nanocomposite [15]. However, in best of our knowledge, the synthesis of CdO nanoparticles and its particle size related photocatalytic in photo degradation of methylene blue has not been reported yet. Hence the present study was meant to study the particle size oriented photocatalytic degradation of methylene blue using the cadmium oxide photocatalyst synthesized by the chemical co-precipitation method. After identifying the crystal structure and phase formation, particle size was estimated to study its effect on photo degradation of methylene blue from the optical absorption studies.

## II. Experimental Details

In the co-precipitation method, cadmium acetate dihydrate  $[(\text{CH}_3\text{COO})_2\text{Cd}\cdot 2\text{H}_2\text{O}]$  was used as the metal salt precursor. In order to hydrolyze the metal salt precursors, ammonium hydroxide  $[\text{NH}_4\text{OH}]$  was added drop-wise to 0.5 M cadmium acetate dihydrate under constant stirring until the pH value of the solution attains 8. To remove the impurities, the resulted precipitate was filtered and washed repeatedly using double distilled water after 18 to 20 hours. The as-prepared cadmium hydroxide was then calcined at different temperatures 400, 600 and 800 °C for 2h to produce nanocrystalline powders of different size and morphology. Possible reaction may be,



Favorable calcination temperature for the formation of crystalline CdO was confirmed by heating (10 °C/minute) the precursor and the samples in Netzsch Thermal Analyzer. X-ray diffraction pattern was recorded in PANalytical X'pert-pro instrumentation using continuous scanning (step size = 0.05 °) with small time constant (step time = 10.138 s). Morphological and microscopic studies have been performed with a PHILIPS CM 200 Model transmission electron microscope. Optical absorbance of the nanopowder was recorded in the ultraviolet, visible and near infra red region using Varian Cary-5000 spectrophotometer. Photocatalytic property of CdO was investigated by mixing 300 mg of the CdO nanoparticles in 50 ml methylene blue aqueous solution with an initial concentration of  $0.5 \times 10^{-5}$  mol/L. The photodegradation of the dye was monitored in a Varian Cary-5000 UV spectrophotometer.

## III. Results And Discussion

### 3.1 Thermal analysis

In order to explore the decomposition pattern of the precursor and to determine the temperature range at which it decomposes to CdO, thermal gravimetric (TG) and differential thermal analysis (DTA) were conducted on the starting precursor (Fig. 1). Decomposition of the starting precursor begins at about 70 °C. The initial weight loss ~14.0 % was observed in TGA curve between 70-150 °C, which corresponds to the removal of two molecules of water in the cadmium acetate dihydrate precursor. Dehydration of  $\text{Cd}(\text{CH}_3\text{COO})_2\cdot 2\text{H}_2\text{O}$  is a two-stage process with  $\text{Cd}(\text{CH}_3\text{COO})_2\cdot \text{H}_2\text{O}$  as intermediate [16], which can be evidenced from the observed two endothermic peaks in the DTA curve. The second mass loss stage is observed in the temperature range 235-328 °C which may be attributed to the decay of the organic components in the precursor structure. The way of  $\text{Cd}(\text{CH}_3\text{COO})_2$  decomposition strongly depends on the surrounding gas atmosphere and the rate of heating. CdO, acetone and  $\text{CO}_2$  are the primary products of decomposition in air [17]. The two sharp endothermic peaks observed at 251 °C and 294 °C in the DTA spectrum corresponding to the second step of the TGA, confirms that sample absorbs heat at these temperatures for the formation of cadmium carbonate ( $\text{CdCO}_3$ ) by the release of acetone ( $\text{C}_3\text{H}_6\text{O}$ ). It was found that the weight loss, as a result of thermal decomposition, ends at about 500 °C, by the release of  $\text{CO}_2$ . Therefore, this temperature was determined as the calcination temperature to reach the metal oxide phase by using the precursor alone. The solid residue formed at around 500 °C is suggested to be CdO. TGA spectrum of the as synthesized powder dried at 100 °C illustrates one step of the mass decay. From 160 - 225 °C, there is about 11 % weight loss in the initial weight, which is equivalent to the loss of one water molecule from each of the  $\text{Cd}(\text{OH})_2$  molecules. The sharp endothermic peak at 215 °C in the DTA spectrum is thus due to the transition of  $\text{Cd}(\text{OH})_2$  into CdO, that happens because of absorption of heat by the sample. There after no other phase transition of CdO was shown by TG-DTA. The studies thus confirmed that the calcination temperature required for the formation of CdO from cadmium acetate is more (>500 °C) compared to the transition from  $\text{Cd}(\text{OH})_2$  (>200 °C). A very minute loss of weight of ~7.0 % in the temperature range 140 °C – 200 °C was observed in TGA spectrum with an endothermic peak in this range in the DTA spectrum of CdO calcined at 400 °C. The endothermic peak at 180 °C shows that the sample absorbs heat at this temperature and liberates the adsorbed water molecule in the sample. Study further suggested the need of calcination at higher temperatures. Hence the as-prepared samples were calcined at 600 and 800 °C also.

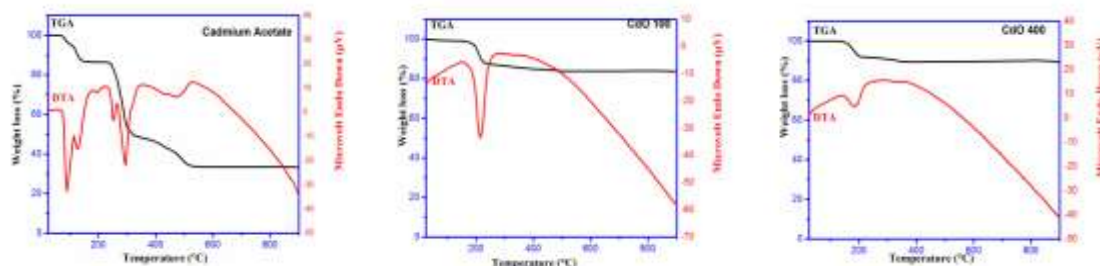


**Fig. 1** TG-DTA curve of cadmium acetate precursor, as-prepared cadmium hydroxide and cadmium oxide calcined at 400 °C

Thus in the present work, in order to explore the properties of CdO nanoparticles for its propriety as a photocatalyst, the thermal analysis encouraged us to chose the starting precursors as cadmium acetate and ammonium hydroxide to form the as prepared cadmium hydroxide for which the calcination temperature required is low as well as the calcination temperatures were chosen as 400, 600 and 800 °C, for the formation of CdO nanoparticles.

### 3.2 X-ray diffraction studies

Fig. 2 shows the XRD spectrum of as-prepared Cd(OH)<sub>2</sub> nanoparticles. The peak positions were compared with the JCPDS standards (JCPDS card no.: 73-0969) for its hexagonal structure and the correct Miller indices to each peak was assigned by indexing the diffraction pattern [18]. The lattice parameters ‘a’ and ‘c’ are estimated and are listed in Table 1. The observed “d” spacings and the relevant prominent peaks for the calcined CdO nanoparticles correspond to reflections of (111), (200), (220), (311) and (222) planes and are in good concord with the standard data (JCPDS card no.: 75-0593). Nonappearance of additional peaks indicates the purity of the prepared samples. Since the Miller indices of the reflections are all odd or all even i.e., unmixed [18], XRD spectra reveal the polycrystalline character of the calcined nanoparticles with cubic (fcc) structure. It is obvious that the lattice structure of as-prepared Cd(OH)<sub>2</sub> particles are hexagonal, which on calcination transform the structure to cubic (fcc). Similar phase transition was reported by Tandra Ghoshal *et al.* [19] where they prepared the samples using solvothermal process. Moreover, it is seen that the lattice parameter of CdO particles gradually decreases on increasing the calcination temperature (Table 1). It indirectly shows the occurrence of compressive strain in the lattice. The unit cell volume of the CdO particles are almost more than double the value of Cd(OH)<sub>2</sub>. So the CdO lattice can be used for doping with other metal ions that can be accommodated in the interstitial positions to tune all the properties of the material.

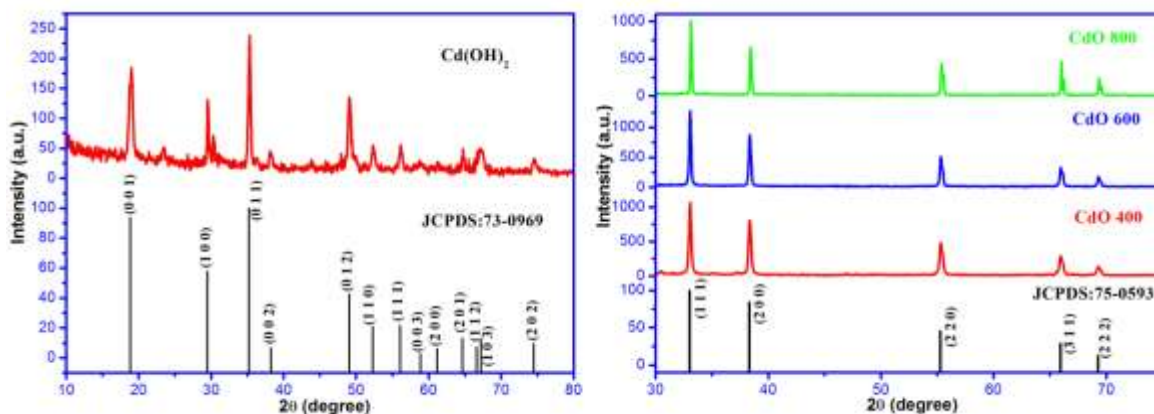


Fig. 2 XRD spectra of as-prepared Cd(OH)<sub>2</sub> and CdO nanoparticles calcined at 400, 600 and 800 °C

Table 1: Structural parameters of as-prepared Cd(OH)<sub>2</sub> and CdO nanoparticles

Sample Details	Lattice Parameter Å		Unit Cell Volume Å <sup>3</sup>		Density g/cm <sup>3</sup>	
	Obs.	Std.	Obs.	Std.	Obs.	Std.
Cd(OH) <sub>2</sub>	a=3.4896 c=4.7053	a=3.496 c=4.702	49.6214	49.77	4.8984	4.885
CdO 400	a=4.6937	a=4.69582	103.4034	103.55	8.2458	8.237
CdO 600	a=4.6925	a=4.69582	103.3281	103.55	8.2518	8.237
CdO 800	a=4.6852	a=4.69582	102.8442	103.55	8.2906	8.237

The crystallite size of CdO was found by the X-ray line broadening technique using the Scherrer equation [20]:

$$D = \frac{0.94 \lambda}{\beta_D \cos \theta} \tag{1}$$

where k is the shape factor used to correlate the size of crystallites to the broadening of a peak in a diffraction pattern, λ is the x-ray wavelength, β<sub>D</sub> is the line broadening at half the maximum intensity (FWHM) in radians, and θ is the Bragg angle, D is the mean size of the ordered (crystalline) domains, which may be smaller or equal to the grain size. In the Williamson-Hall technique, crystallite size D and micro strain ε are related and the slope of the plot between 4sinθ and β<sub>D</sub>cosθ gives the microstrain and the crystallite size value [21]. The crystallite size determined from the Scherrer and the Williamson-Hall analysis are presented in Table 2 which shows a greater disparity because of the variation in averaging the crystallite size distribution. The crystallite size increases as

the calcination temperature increases but strain value decreases and it is found that the strain arising, as calculated from Williamson-Hall method are very minute and have an insignificant effect on peak broadening. Small-sized nanoparticles with great surface area are proficient substrates for absorption of light [22] which is essential for the enhancement of photocatalytic activity. Moreover, a restrictive factor that reins the competence of photocatalysis is the rapid recombination of photogenerated holes and electrons in the semiconductor particles [23]. Defects in the lattice structure are detrimental to the photocatalytic activity as they act as trap sites for the photogenerated charge carriers, increasing their probability of recombination [24]. In view of these aspects, the prepared nanoparticles for different calcination temperatures with crystallite size in the range 22 nm to 72 nm can act as efficient photocatalysts for the elimination or abatement of environmental pollutants.

**Table 2:** Crystallite Size (D) and Microstrain (ε) Data

Sample Details	Scherrer formula D (nm)	Williamson-Hall plot	
		D (nm)	ε
<b>CdO 400</b>	39.3161	21.6144	-0.00182
<b>CdO 600</b>	60.0885	55.6986	-9.6x 10 <sup>-5</sup>
<b>CdO 800</b>	107.254	72.0480	-3.5 x 10 <sup>-4</sup>

By indexing the X-ray diffraction pattern to the crystal planes of cubic CdO and by calculating the texture coefficient (TC) for each particular crystal plane from the relative intensity using Eq. (3) [25], the crystal orientation transition is quantified in Table 3.

$$TC(hkl) = \frac{I(hkl)}{I_0(hkl)} \left( \frac{1}{n} \sum_{i=1}^n \frac{I(hkl)}{I_0(hkl)} \right)^{-1} \tag{2}$$

where, I is the relative intensity of reflection from a measured plane (hkl), I<sub>0</sub> is the standard intensity of reflection of the same plane taken from the JCPDS file no. 75-0593 and n is the total number of measured reflection peaks used and is equal to 5 for the samples listed in Table 3. Thus, a TC of 5 describes a perfect orientation whereas a perfectly random orientation in all the reflecting planes would have a TC of 1. For a preferential orientation, the texture coefficient TC (hkl) should be greater than one [26]. Of all the samples, the preferred orientation along the (111) diffraction plane is more noticeable. This indicates no phase change in the prepared CdO nanoparticles during different calcinations.

**Table 3:** Calculated texture coefficient values

Planes	1 1 1	2 0 0	2 2 0	3 1 1	2 2 2
<b>CdO400</b>	1.850892	1.495521	0.945436	0.495114	0.213038
<b>CdO600</b>	1.952667	1.269624	0.860736	0.602203	0.31477
<b>CdO800</b>	1.736352	1.069246	0.90134	0.85498	0.438082

### 3.4 TEM Analysis

The TEM image for CdO nanoparticles calcined at 400 and 800 °C are shown in Fig. 3 which indicates that the morphology of CdO powder consists of hexagonal and spherical crystals. The well-defined CdO nanoparticles calcined at 400 °C, as seen from the TEM micrograph have an average diameter of about 47.54 nm. The transmission electron micrograph of CdO nanoparticles calcined at 800 °C shows a network of large particles of moderate sizes formed by agglomeration of well dispersed nanoparticles with the average size of 72 nm. The sizes of these nanoparticles are in good accord with the values obtained from XRD experiment. Furthermore the special morphology with round edges and corners has more active sites in the photocatalytic process and hence shows high photocatalytic activity during the process of degradation of organic pollutant in aqueous solution [27]. Therefore the particular hexagonal and spherical morphology of CdO nanoparticles obtained in the present study, with number of round edges and corners, have more active sites that promote the photocatalytic activity of CdO. The polycrystalline nature of the obtained samples was confirmed by selected area electron diffraction (SAED). The radii r of the diffraction circles is related to the d-spacing by the relation [28]:

$$d = \frac{L\lambda}{r} \tag{3}$$

The observed “d” spacings for the particular “r” values match to (111), (200), (220), (311) and (222) planes and are in good concord with the standard data (JCPDS card no.: 75-0593), for the polycrystalline character of the calcined CdO nanoparticles with cubic (fcc) structure.

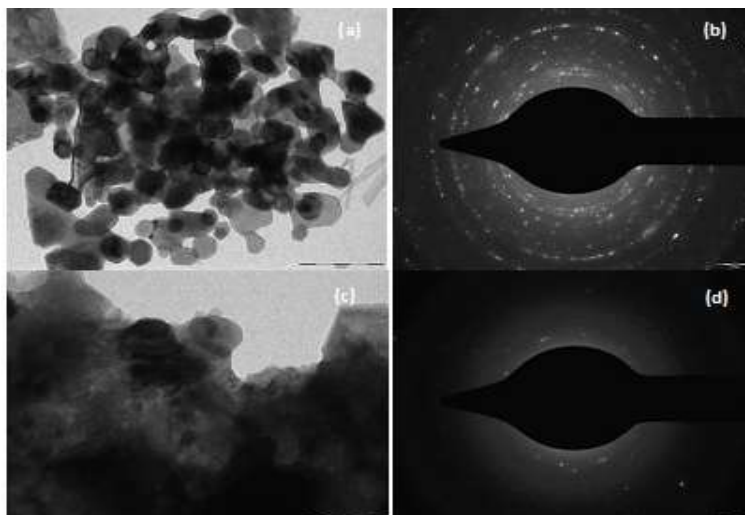


**Fig. 3** TEM images and SAED pattern of CdO nanoparticles calcined at 400 and 800 °C

### 3.5 Optical study

The optical band gap ( $E_g$ ) of a semiconductor is connected to the optical absorption coefficient ( $\alpha$ ) and the incident photon energy ( $h\nu$ ) by equation (5) [29]:

$$(\alpha h\nu) = (E_g - h\nu)^n \quad (4)$$

where  $n$  is an index which assumes the values of 1/2, 3/2, 2 and 3 depending on the nature of the electronic transition accountable for the absorption. Specifically, when the transition is directly and indirectly allowed,  $n$  is 1/2 and 2 respectively. According to theoretical and experimental results, CdO show direct interband transitions [30]. Thus  $n$  can be chosen as 1/2. For the optical band gap of CdO nanoparticles calculation,  $(\alpha h\nu)^2$  vs.  $h\nu$  curve was plotted and linear portion of the curve was then extrapolated to  $(\alpha h\nu)^2 = 0$ . Fig. 4 illustrates the plots between  $(\alpha h\nu)^2$  vs.  $h\nu$  for CdO nanoparticles, thus indicates the optical band gap variation of CdO nanoparticles with various calcination temperatures. The optical band gap of the CdO nanoparticles calcined at 400, 600 and 800 °C seems to be 2.49 eV, 2.27 eV and 2.17 eV respectively. It has also seen that  $E_g$  of CdO nanoparticles decreases with increasing calcination temperature, which could arise from improvements in morphological and crystallinity of the samples, as supported by XRD studies. Furthermore change in the optical band gap of the nano-structured materials can be elucidated based on quantum size effect; smaller the size of the crystal, the higher the band gap. Thus the shifting of optical absorption edge towards smaller energy with increase in calcination temperature from 400 to 800 °C, is ascribed to an increase in size of grain at higher calcination temperatures [31]. Calcination at higher temperatures is known to decrease the number of oxygen vacancies [32] and thus the band gap of CdO nanoparticles decreases with higher calcination temperatures. Titania is known to be the best photocatalyst with a wide band gap  $\sim 3$  eV [33]. Despite several advantages like easy availability, high surface areas, high chemical stability, environmental friendliness etc, it's worth is condensed such that it displays photoactivity only under UV light (wavelength  $< 400$  nm) and it will not utilize light of energies  $< 3$  eV. As visible light accounts for 43% of solar energy, the dispute lies in design and progress of efficient photocatalysts of band gaps  $< 3$  eV with efficiencies analogous to  $\text{TiO}_2$ . One of the basic requirements of an ideal photocatalyst is an optical band gap around 2.0 eV for absorption of the maximum portion of visible light [34]. The obtained band gap that ranges from 2.2 eV to 2.5 eV are thus accountable for the higher photocatalytic activity of the prepared nanopowders.

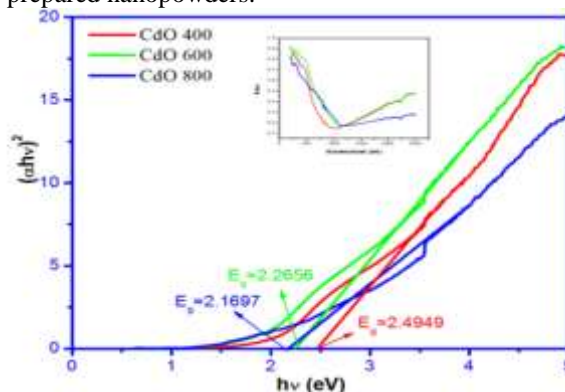


**Fig. 4** Plot of  $(\alpha h\nu)^2$  vs  $h\nu$  with UV-Vis absorption spectra in the inset

### 3.6 Photocatalytic study

Encouraged by the competence of the visible light absorption, we further inspected the viability of these prepared CdO nanopowders as a visible light driven photocatalyst in the degradation of organic pollutants. Methylene blue (MB), as a widespread dye in textile industry, was chosen as the organic contaminant. Fig. 5 shows the MB absorption spectra in the range 500–750 nm, obtained before and after 1, 2, 3 and 4 h of light irradiation in presence of the prepared CdO samples and was examined that the intensity of the absorption bands diminishes as the irradiation time increases. Starting from these absorption spectra, the [MB] normalized as a function of time (h) (Fig. 6) has nearly an exponential decay, feature of a first order reaction:  $[MB] = [MB]_0 e^{-kt}$ , where k is the rate constant,  $[MB]_0$  is the initial MB concentration, and [MB] is the MB concentration after time t. The kinetics of disappearance of MB with time obeys pseudo-first-order kinetics [35], the slope of which gives the rate constant k. k value was found to be  $0.3 \text{ hr}^{-1}$  for all the prepared samples, which proves the best photocatalytic activity of CdO nanoparticles that make it a workable substitute for the elimination of color from textile waste water. The kinetic results also show that a decline in the MB concentration results in an increase in the obvious photocatalytic activity of the CdO nanoparticles. The entire photocatalytic process depends on the properties of the catalyst, and the effective light intensity in the system. Small-sized nanoparticles with great surface area are proficient substrates for absorption of light [36] which is essential for the enhancement of photocatalytic activity. It was obvious from the that the sample calcined at  $400^\circ\text{C}$  shows the best photocatalytic activity with k value of  $0.3474 \text{ h}^{-1}$ . This should be ascribed to the enhancement of the semiconducting property of CdO with lesser particle size that led to the stronger interaction between dye molecules and nanoparticles. Due to this the CdO nanoparticles calcined at  $400^\circ\text{C}$  had the strongest degradation capability compared with others and the capability can be determined using the formula:

$$\% \text{Degradation} = \frac{A_{\max} - A}{A_{\max} - A_{\min}} \times 100 \quad (5)$$

Where

- A is the value of the absorption at a particular time t
- $A_{\max}$  is the maximum value of the absorption
- $A_{\min}$  is the minimum value of absorption [33]

In fact, the percentage of degradation of MB in presence of CdO photocatalysts calcined at 400, 600 and  $800^\circ\text{C}$  are found to be 71, 62 and 57% respectively, in 5 hours of the reaction according to the above relation.

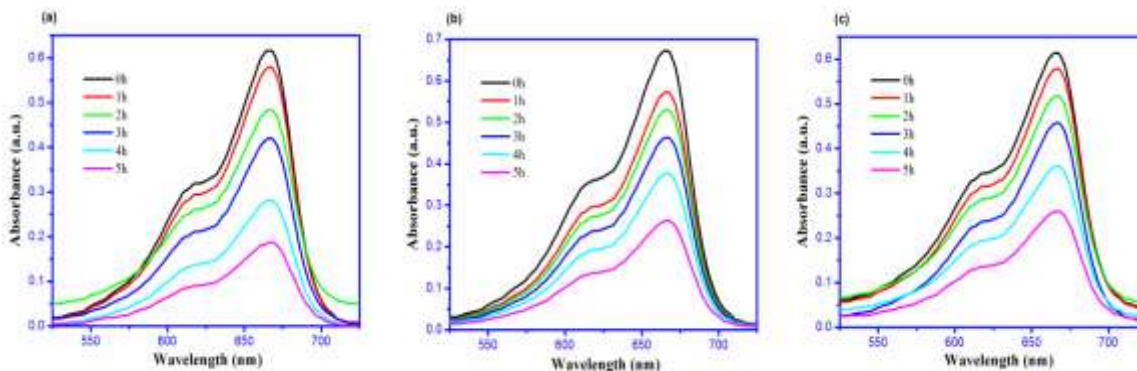


Fig. 5 MB absorption spectra at different times of irradiation in presence of CdO800 photocatalyst

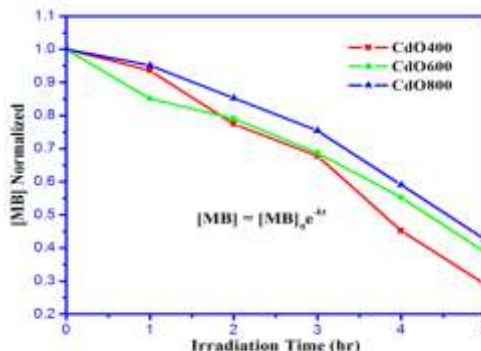


Fig. 6 [MB] normalized as a function of time

#### IV. Conclusion

Nano-sized cadmium oxide powders for different calcination temperatures were successfully synthesized using chemical co-precipitation method which is a simple, cost-effective and quick method for the synthesis of CdO nanospheres. Thermal analysis shows that the final decomposition temperature of the acetate precursor starts around 350 °C for the formation of CdO. The low temperature endothermic decomposition of the carbonaceous material present in the precursor reduces the processing temperature for the preparation of fine particles of this oxide system. The as-prepared Cd(OH)<sub>2</sub> powder samples crystallizes to its hexagonal structure whereas on calcination at 400, 600 and 800 °C transform it to cubic CdO. It was observed that the calcination temperature has major influence on structural parameters evaluated from the recorded XRD spectra. The line broadening in XRD peaks because of tiny crystallite size and lattice strain were studied by Scherrer formula and Williamson-Hall plots. The size of these nanoparticles as seen from TEM images matched well with the values obtained from XRD. Optical absorption in the UV-Vis spectra of the cadmium nano oxides indicated decrease in direct band gap with calcination temperature and the decreased values remained wide. Investigations further hoisted the photocatalytic activity of CdO towards color degradation and advocated the suitability of CdO as a viable alternative for the removal of color from textile waste water.

#### References

- [1]. M. Ajmal, A.U. Khan, Effects of a textile factory effluent on soil and crop plants environmental pollution, *Environ. Pollut. Ser. A.*, 37, 1985, 131 -148.
- [2]. M. Ghaedi, A. Ansari, M.H. Habibi, A.R. Asghari, Removal of malachite green from aqueous solution by zinc oxide nanoparticle loaded on activated carbon: Kinetics and isotherm study, *J. Indus. Engineer. Chem.*, 20 (1), 2014, 17 - 28.
- [3]. S.T. Hung, C.J. Chang, M.H. Hsu, Improved photocatalytic performance of ZnO nanograss decorated pore-array films by surface texture modification and silver nanoparticle deposition, *J. Hazard. Mater.*, 198, 2011, 307 - 316.
- [4]. Sana Akir, Alexandre Barras, Yannick Coffinier, Mohamed Bououdina, Rabah Boukherroub, Amel Dakhlaoui Omrani, Eco-friendly synthesis of ZnO nanoparticles with different morphologies and their visible light photocatalytic performance for the degradation of Rhodamine B, *Ceramic International*, 42, 2016, 10259 - 10265.
- [5]. Ganesh Elango, Selvaraj Mohana Roopan, Efficacy of SnO<sub>2</sub> nanoparticles toward photocatalytic degradation of methylene blue dye, *Photochem. Photobiol.*, 155, 2016, 34 - 38.
- [6]. A. Sarkar, A. Shchukarev, A.R. Leino, K. Kordas, J.P. Mikkola, P.O. Petrov, E.S. Tuchina, A.P. Popov, M.E. Darvin, M.C. Meinke, J. Lademann, V.V. Tuchin, Photocatalytic activity of TiO<sub>2</sub> nanoparticles: effect of thermal annealing under various gaseous atmospheres, *Nanotechnology*, 23, 2012, 475711 (8pp).
- [7]. A. Callegari, D. Tonti, M. Chergui, Photochemically Grown Silver Nanoparticles with Wavelength-Controlled Size and Shape, *Nano Lett.*, 3 (11), 2003, 1565 - 1568.
- [8]. Y.J. Huang, D.H. Kim, Light-controlled synthesis of gold nanoparticles using a rigid, photoresponsive surfactant, *Nanoscale*, 4, 2012, 6312 - 6317.
- [9]. S. Kundu, K. Wang, S. Lau, H. Liang, Photochemical synthesis of shape-selective palladium nanocubes in aqueous solution, *J. Nanopart. Res.*, 12 (8), 2010, 2799 - 2811.
- [10]. S. Kundu, H. Liang, Photoinduced Formation of Shape-Selective Pt Nanoparticles, *Langmuir*, 26 (9), 2010, 6720 - 6727.
- [11]. R. Kumar, Ahmad Umar, G. Kumar, M.S. Akhtar, Yao Wang, S. H. Kim, Ce-doped ZnO nanoparticles for efficient photocatalytic degradation of direct red-23 dye, *Ceramic International*, 41 (6), 2015, 7773 - 7782.
- [12]. Phendukani Ncube Ndzonelelo Bingwa Hajecarim Baloyi Reinout Meijboom, Catalytic activity of palladium and gold dendrimer-encapsulated nanoparticles for methylene blue reduction: A kinetic analysis, *Appl. Catalysis A.*, 495, 2015, 63 - 71.
- [13]. P. Hemalatha, S.N. Karthick, K.V. Hemalatha, Moonsuk Yi, Hee-Je Kim, M. Alagar, La-doped ZnO nanoflower as photocatalyst for methylene blue dye degradation under UV irradiation, *J. Mat. Sci.: Mat. in Electronics.*, 27 (3), 2016, 2367 - 2378.
- [14]. R. Saravanan, M. Mansoob Khan, V.K. Gupta, E. Mosquera, F. Gracia, V. Narayanan, Stephen, ZnO/Ag/CdO Nanocomposite for Visible Light-Induced Photocatalytic Degradation of Industrial Textile Effluents, *J. Colloid Interface Sci.*, 452, 2015, 126 - 133.
- [15]. Handan Gülce, Volkan Eskizeybek, Bircan Haspulat, Fahriye Sari, Ahmet Gülce, Ahmet Avci, Preparation of a New Polyaniline/CdO Nanocomposite and Investigation of Its Photocatalytic Activity: Comparative Study under UV Light and Natural Sunlight Irradiation, *Indus. Engineer. Chem. Res.*, 52, 2013, 10924 - 10934.
- [16]. Azadeh Tadjarodi, Mina Imani, Hamed Kerdari, Application of a facile solid-state process to synthesize the CdO spherical nanoparticles, *International Nano Letters*, 3, 2013 :43 (1 - 6).
- [17]. Barbara Malecka, Thermal decomposition of Cd(CH<sub>3</sub>COO)<sub>2</sub>·2H<sub>2</sub>O studied by a coupled TG-DTA-MS method, *J. Therm. Anal. Calorim.*, 78 (2), 2004, 535 - 544.
- [18]. C. Suryanarayana, M. Grant Norton, X-ray Diffraction: A Practical Approach, New York, 1998.
- [19]. Tandra Ghoshal, Soumitra Kar, Subhadra Chaudhuri, Synthesis of nano and micro crystals of Cd(OH)<sub>2</sub> and CdO in the shape of hexagonal sheets and rods, *Appl. Surf. Sci.*, 253, 2007, 7578 - 7584.
- [20]. K. Gurumurugan, D. Mangalaraj, S.K. Narayandass, Magnetron sputtered transparent conducting CdO thin films, *J. Electron. Mater.*, 25 (5), 1996, 765 - 770.
- [21]. T. Fernandez, G. Jose, S. Mathew, P.R. Rejikumar, N.V. Unnikrishnan, An ultra-low hydrolysis sol-gel route for titanosilicate xerogels and their characterization, *Sol-Gel Sci. Technol.*, 41 (2), 2007, 163 - 168.
- [22]. L. Wang, L. Chang, B. Zhao, Z. Yuan, G. Shao, and W. Zheng, Systematic investigation on morphologies, forming mechanism, photocatalytic and photoluminescent properties of ZnO nanostructures constructed in ionic liquids, *Inorg. Chem.*, 47, 2008, 1443 - 1452.
- [23]. D. Robert, Photosensitization of TiO<sub>2</sub> by M<sub>x</sub>O<sub>y</sub> and M<sub>x</sub>S<sub>y</sub> nanoparticles for heterogeneous photocatalysis applications, *Catal. Today.*, 122 (1 - 2), 2007, 20 - 26.
- [24]. O. Carp, C.L. Huisman, A. Reller, Photoinduced Reactivity of Titanium Dioxide, *Prog. Solid State Chem.*, 32, 2004, 33 - 177.
- [25]. C. S. Barrett, T.B. Massalski, *Structure of Metals*, Pergamon, Oxford, 1980, p. 204
- [26]. K. Gurumurugan, D. Mangalaraj, S.K. Narayandass, K. Sekar, C.P. Giriya Vallabhan, Characterization of transparent conducting CdO films deposited by spray pyrolysis, *Semicond. Sci. Technol.*, 9, 1994, 1827 - 1832.

- [27]. Songwang Yang, Lian Gao, Preparation of titanium dioxide nanocrystallite with high photocatalytic activities, *J. Am. Ceram. Soc.*, 88, 2005, 968 - 970.
- [28]. Shugang Wang, Yaoxian Li, Jie Bai, Qingbiao Yang, Yan Song, Chaoqun Zhang, Characterization and photoluminescence studies of CdTe nanoparticles before and after transfer from liquid phase to polystyrene, *Bull. Mater. Sci.*, 32, 2009, 487 - 491.
- [29]. C.G. Granqvist, Electrochromic tungsten oxide films: Review of progress 1993–1998, *Sol. Energy Mater. Sol. Cells.*, 60 (3), 2000, 201 - 262.
- [30]. S. Aksoy, Y. Caglar, S. Ilican, M. Caglar, Effect of heat treatment on physical properties of CdO films deposited by sol–gel method, *Int. J. Hydrogen Energy*, 34, 2009, 5191 - 5195.
- [31]. S.A. Vanalakar, S.S. Mali, M.P. Suryavanshi, P.S. Patil, Quantum size effect in chemosynthesized nanostructured CdS thin films, *Dig. J. Nanomater. Bios.*, 5, 2010, 805 - 810.
- [32]. Y. Dou, T. Fishlock, R.G. Egdell, D.S.L. Law, G. Beamson, Band-gap shrinkage in n-type-doped CdO probed by photoemission spectroscopy, *Phys. Rev. B.*, 55, 1997, 381 - 384.
- [33]. V. Yu., Kolenko, B.R. Churagulov, M. Kunst, L. Mazerolles, C. Colbeau-Justin, Photocatalytic properties of titania powders prepared by hydrothermal method, *Appl. Catal., B: Environmental*, 54, 2004, 51 - 58.
- [34]. Jiajia Wang, Tao Fang, Li Zhang, Jianyong Feng, Zhaosheng Li, Zhigang Zou, Effects of oxygen doping on optical band gap and band edge positions of Ta<sub>3</sub>N<sub>5</sub> photocatalyst: A GGA + U calculation, *J. Catal.*, 309, 2014, 291 - 299.
- [35]. Alamgir, WasiKhan, Shabbir Ahmad, A.H. Naqvi, Formation of self-assembled spherical-flower like nanostructures of cobalt doped anatase TiO<sub>2</sub> and its optical band-gap, *Mater. Lett.*, 133, 2014, 28 - 31.
- [36]. L. Wang, L. Chang, B. Zhao, Z. Yuan, G. Shao, and W. Zheng, Systematic Investigation on Morphologies, Forming Mechanism, Photocatalytic and Photoluminescent Properties of ZnO Nanostructures Constructed in Ionic Liquids, *Inorg. Chem.*, 47 (5), 2008, 1443 - 1452.

IOSR Journal of Applied Physics (IOSR-JAP) is UGC approved Journal with SI. No. 5010, Journal no. 49054.

D.J. Jeejamol. "CdO Nanoparticles: Facile Synthesis and Influence of Particle Size on Photocatalytic Degradation of Methylene Blue ." *IOSR Journal of Applied Physics (IOSR-JAP)*, vol. 9, no. 5, 2017, pp. 66–73.